Peptide-coated semiconductor nanocrystals for biomedical applications

X. Michalet[*], F. F. Pinaud, L.A. Bentolila, J. M. Tsay, S. Doose[‡], J. J. Li, G. Iyer, S. Weiss[†]

Dpt of Chemistry & Biochemistry, UCLA
607 Charles E. Young Drive East, Los Angeles, CA 90095
[‡] Applied Laserphysics & Laserspectroscopy, University of Bielefeld
33615 Bielefeld, Germany

ABSTRACT

We have developed a new functionalization approach for semiconductor nanocrystals based on a single-step exchange of surface ligands with custom-designed peptides. This peptide-coating technique yield small, monodisperse and very stable water-soluble NCs that remain bright and photostable. We have used this approach on several types of core and core-shell NCs in the visible and near-infrared spectrum range and used fluorescence correlation spectroscopy for rapid assessment of the colloidal and photophysical properties of the resulting particles. This peptide coating strategy has several advantages: it yields probes that are immediately biocompatible; it is amenable to improvements of the different properties (solubilization, functionalization, etc) via rational design, parallel synthesis, or molecular evolution; it permits the combination of several functions on individual NCs. These functionalized NCs have been used for diverse biomedical applications. Two are discussed here: single-particle tracking of membrane receptor in live cells and combined fluorescence and PET imaging of targeted delivery in live animals.

KEYWORDS

quantum dots, nanocrystal, fluorescence, photophysics, single-molecule, peptide, functionalization, live cell, FCS

1. INTRODUCTION

Fluorescent semiconductor nanocrystals (NCs)[3] have become increasingly popular as potential replacement of fluorescent dyes for multiple biomedical applications. Their broad excitation spectra, associated with tunable and narrow emission spectra, their photostability, brightness and quantum yield make them serious contenders as ideal fluorescent probes for applications demanding high-sensitivity, high signal-to-noise or long observations[4]. However, high-quality NCs are usually synthesized in organic solvents, and additional chemical modifications are required to solubilize them in aqueous buffers and functionalize them for biomedical applications. This is accomplished by exchanging the hydrophobic surface ligands with amphiphilic ones. Different NC solubilization strategies have been devised over the past few years, including: (*i*) ligand exchange with simple molecules such as mercaptoacetic acid[5], dithiothreitol[6] or more sophisticated ones such as oligomeric phosphines[7], dendrimers[8], amphiphilic polymers[9] triblock copolymers[10] and peptides[1], (*ii*) encapsulation in silica shells[11, 12], phospholipid micelles[13], polymer beads[14], polymer shells[15], amphiphilic polysaccharides[16] and, (*iii*) combination of several layers conferring the required colloidal stability to NCs[17-19]. Among these possible routes, some have known limitations, leading to particles that either lack long-term stability[5, 6], have reduced QY, are significantly larger than the original particles[9, 10], have broader size distributions[11] or do not work well with all particle sizes[13]. Recently, some groups have developed promising water-based synthesis[20, 21] yielding particles emitting from the visible to the NIR spectrum that are natively water-soluble, but have yet to be tested in biological environments.

[*] michalet@chem.ucla.edu
[†] sweiss@chem.ucla.edu

Genetically Engineered and Optical Probes for Biomedical Applications III,
edited by D. J. Bornhop, S. I. Achilefu, R. Raghavachari, A. P. Savitsky, Proc. of SPIE
Vol. 5704 (SPIE, Bellingham, WA, 2005) · 1605-7422/05/$15 · doi: 10.1117/12.589498

Solubilization is but the first step towards using NCs as biological probes, unless they are used as mere non-specific fluorescent stain, as demonstrated in experiment involving *E. coli* bacteria[22], amoeba[23] and human cell lines[23-25] or *Xenopus* embryo[13]. For biological targeting, some kind of biological "interfacing" is necessary. Some applications will require having a single recognition moiety attached to the nanocrystal (e.g. DNA oligonucleotide, aptamer, antibody, etc). A simple method consists of exchanging the solubilization ligands with the molecule of interest, as was demonstrated with DNA oligonucleotides [26]. More generally, as most NC-ligands expose either a carboxyl or an amine group, standard bioconjugation reactions can be used to functionalize NCs with molecules containing a thiol group[13, 27, 28] or an NHS-ester moiety[11] respectively. Alternatively, heterobifunctional reagents [5-7, 19, 29] can be used to cross-link molecules to the NC-ligands. Avoiding functionalization chemistry altogether, some researchers have used electrostatic interactions between NCs and charged adapter molecules, or proteins modified to incorporate charged domains[30, 31]. For instance, biotinylated or streptavidin- (SAv) coated NCs can be used in combination with SAv-functionalized or biotinylated proteins or antibodies[1, 9, 17, 23, 32-35]. Using an antibody against a specific target, and a biotinylated secondary antibody, itself bound to a SAv-coated NC, any type of target can be labeled using a three-layer approach [9, 34].
In contrast to classical fluorophores used for biological labeling, the large surface area of NCs (their diameter varying from a few nm[36] to a few dozens nm[10]) increases the number of available attachment groups (10-100). In other words, labeling of NCs is therefore statistical and conrolled by stoichiometry. If the size of the attached moiety approaches the

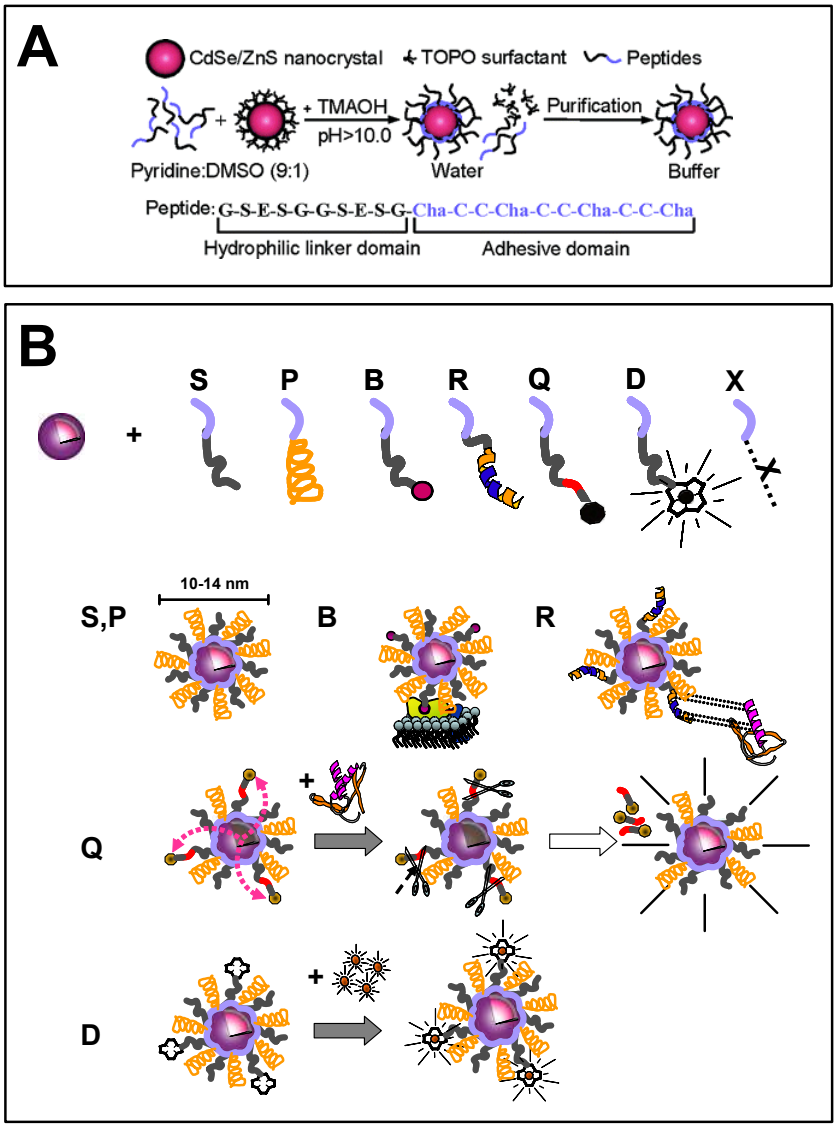

Fig. 1: Nanocrystal peptide-coating approach. A. Schematic representation of the surface coating chemistry of CdSe/ZnS nanocrystals with phytochelatin-related [illegible]-peptides. The peptide C-terminal adhesive domain binds to the ZnS shell of CdSe/ZnS nanocrystals after exchange with the trioctylphosphine oxide (TOPO) surfactant. A polar and negatively charged hydrophilic linker domain in the peptide sequence provides aqueous buffer solubility to the nanocrystals. TMAOH: Tetramethyl ammonium hydroxide; Cha: 3-cyclohexylalanine. From ref. [1]. B. Peptide toolkit. The light blue segment contains cysteines and hydrophobic aminoacids ensuring binding to the nanocrystal (adhesive domain of Fig. 1A) and is common to all peptides. S: solubilization sequence (hydrophilic linker domain of Fig. 1A), P: PEG, B: biotin, R: recognition sequence, Q: quencher, D: DOTA (1,4,7,10-tetraazacyclododecane-1,4,7,10-tetraacetic acid) for radionuclide and nuclear spin label chelation, X: any unspecified peptide-encoded function. NCs solubilization is obtained by a mixture of S and P. NCs can be targeted with biotin (B), a peptide recognition sequences (R), or other chemical moieties. NCs fluorescence can be turned on or off by attaching a quencher (Q) via a cleavable peptide link. In the presence of the appropriate enzyme, the quencher is separated from the NC, restoring the photoluminescence and reporting on the enzyme activity. For simultaneous PET (resp. MRI) and fluorescence imaging, NCs can be rendered radioactive by chelation of radionuclides (resp. nuclear spin labels) using DOTA (D). Adapted from ref. [4].

NC size, steric hindrance will prevent the attachment of more than a few of these moieties per NC. Size or charge differences can sometimes be utilized to further purify singly labeled from unlabeled or multiply labeled NCs. In some cases, multipotent NC probes can be desirable. The large number of surface attachment groups becomes an advantage, as different functions can be "grafted" to individual NCs. For instance, in addition to a recognition moiety, NCs could be equipped with a membrane crossing or cell internalization capability, and/or an enzymatic function. In general however, addition of functions may result in an increase of the final NC size.Our group has investigated a new approach that would allow a single type of ligand and a single step exchange of surfactant to perform all necessary functions: (i) protect the core-shell NC from degradation, (ii) maintain the original NC photophysical properties, (iii) solubilize NCs in aqueous buffers (iv) provide a biological interface to the NC, and (v) allow multiple functions to be easily incorporated. This surface chemistry was designed to be simple, robust, and evolvable. The existence of biologically synthesized NCs[37] consisting of CdS cores coated by natural peptides, led us to rationally design several peptide sequences comprising a metal-chelating part and hydrophobic residues ensuring attachment to the NC shell, and a hydrophilic tail providing solubilization (Fig. 1A). The resulting particles have excellent colloidal properties, photophysics and biocompatibility, and this "peptide toolkit" can easily be tailored to provide additional functionalities (Fig. 1B). More importantly, these peptide-coated NCs are amenable to molecular evolution for improved properties, a strategy that has proven extremely powerful for the recognition, synthesis and self-assembly of nanocrystals[38, 39]. The versatility of the peptide code, and the example of the myriad of functions evolved by Nature, endows this technology with the potential to fulfill the goals previously set forward.

This peptide-coating technique yield small, monodisperse and very stable water-soluble NCs that remain bright and photostable. We have successfully used this approach on several types of core and core-shell NCs in the visible and near-infrared spectrum range. The colloidal and photophysical properties of the resulting particles were tested by fluorescence correlation spectroscopy (FCS) and single-molecule spectroscopy (SMS). In this report, we describe the peptide-coating approach (section 2), the results of colloidal and photophysical characterization for various types of NCs (section 3 & 4), and conclude with two examples of biological applications: single-particle tracking (SPT) of membrane receptor in live cells (section 5) and combined fluorescence and micro-positron emission tomography (μPET) imaging of targeted delivery in live animals (section 6). We conclude by a brief overview of future developments (section 7).

2. THE PEPTIDE-COATING APPROACH

2.1. A natural design

As illustrated by the brief review of available techniques presented in the introduction, interfacing hydrophilic organic molecules with the inorganic surface of NCs is a significant challenge. Interestingly, very efficient processes have naturally evolved for this particular problem in the form of biosynthesis of phytochelatins by some plants, yeast and bacteria strains. Phytochelatins are cysteine-rich peptides that these organisms synthesize to detoxify their environment from harmeful metal ions such as Cd^{2+} [40]. These peptides of structure (γ-EC)$_n$G (n, the number of dipeptide repeats, is typically 2-4) can complex metal ions into semiconductor NCs such as CdS[37, 41]. These intracellular peptide-coated NCs are very stable and possess photoluminescent properties similar to chemically synthesized NCs, but have a tendency to degrade upon photoexcitation[42]. Phytochelatin-related peptides with γ and α-linkages have been used as templates for nucleation and in vitro growth of NCs such as ZnS or CdS[42, 43]. Recently, combinatorial techniques[44, 45] and phage display[38] have been employed to improve the interfacing of peptides with semiconductor nanoparticles. However, NCs grown from peptide templates have found little use as probes for biological imaging. One possible reason is their lower crystalline quality compare to chemically synthesized NCs, but also the absence of higher band gap shell material on top of the semiconductor cores, which might result in rapid photodegradation. On the basis of these naturally formed organic-inorganic hybrid materials, we designed synthetic γ-peptides similar to the phytochelatins, that can efficiently bind on the surface of CdSe/ZnS NCs synthesized with TOPO surfactant and provide buffer soluble, biocompatible, and photostable NCs probes amenable to fluorescence imaging of live cells.

2.2. Amphiphilic peptide sequences

The binding reaction of a typical phytochelatin-related synthetic γ-peptide on CdSe/ZnS NCs synthesized following standard protocols[1] is presented in Fig. 1A. The 20 amino acid long amphiphilic peptide has a hydrophobic adhesive domain that binds on the ZnS surface of the NCs and a negatively charged and hydrophilic linker domain that can be modified to include binding sequences or functional groups for conjugation (Fig. 1B) Cysteinyl thiolates, present in the

adhesive domain, have previously been reported to act as surface ligands on NCs such as CdS and ZnS[41, 46, 47]. Replacement of the cysteine residues (C) by alanine resulted in water insoluble particles, confirming that the essential role of cysteine for the binding of the peptides on the NCs surface. Multiple repeats of cysteine in tandem were preferred so as to enhance the stability of the peptide on the NCs by better surface coverage. Limiting the adhesive domain to one repeat only resulted in unstable NCs. Such length-dependent stability was previously reported for CdS NCs coated with phytochelatin peptides of various lengths[42]. The presence of hydrophobic 3-cyclohexylalanine (Cha) residues around the cysteines in the adhesive domain helped the solubilization of the peptides in an apolar 9:1 (v:v) pyridine:dimethylsulfoxide (DMSO) cosolvent where TOPO-coated NCs are stable, therefore limiting the formation of aggregate during the reaction . The large cyclohexyl moieties were also chosen to limit the cross-reactivity between the cysteines of the adhesive domain and to compete with the hydrophobic TOPO on the NCs surface. When the Cha residues were replaced by alanine, the obtained peptide-coated NCs were unstable in buffers. We have been recently successful in replacing the unnatural amino-acid Cha by a natural one while preserving the stability and photophysical properties of peptide-coated NC (data not shown).

Binding of the peptides on the ZnS layer was initiated by the formation of cysteine thiolates anion with the addition of tetramethylammonium hydroxide (TMAOH) base. Upon binding of the peptides, the nanoparticles precipitate out of the cosolvent, and can be redissolved in DMSO and water. Dialysis and centrifugal filtration were then used to remove the excess of un-bound peptides and the purification was assessed by size exclusion liquid chromatography (SE-HPLC) and SDS-PAGE gel electrophoresis[1].

Designation	NCs solubility Water/Buffer[a]	NCs pH stability 4.0/10.0[b]	Sequences[c]
1	+/-	ND	Cha-C-C-Cha-C-C-Cha-C-C-Cha-**Cmd**
2	+/-	ND	G-G-S-G-G-S-G-G-Cha-C-C-Cha-C-C-Cha-C-C-Cha-**Cmd**
3	-/-	-/-	G-R-R-G-E-G-R-R-G-Cha-C-C-Cha-C-C-Cha-C-C-Cha-**Cmd**
4	+/+	+/+	G-S-E-S-G-G-S-E-S-G-Cha-C-C-Cha-C-C-Cha-C-C-Cha-**Cmd**
5	+/+	+/+	**Ac**-G-S-E-S-G-G-S-E-S-G-Cha-C-C-Cha-C-C-Cha-C-C-Cha-**Cmd**
6	+/+	+/+	**Suc**-G-S-S-S-G-G-S-S-S-G-Cha-C-C-Cha-C-C-Cha-C-C-Cha-**Cmd**
7	+/+	+/+	K-G-S-E-S-G-G-S-E-S-G-Cha-C-C-Cha-C-C-Cha-C-C-Cha-**Cmd**
8	+/+	+/+	Biotin-G-S-E-S-G-G-S-E-S-G-Cha-C-C-Cha-C-C-Cha-C-C-Cha-**Cmd**
9	+/-	+/+	PEG-Cha-C-C-Cha-C-C-Cha-C-C-Cha-**Cmd**
10	+/+	-/+	**Ac**-G-P-K-K-K-R-K-V-G-G-S-E-S-G-G-S-E-S-G-Cha-C-C-Cha-C-C-Cha-C-C-Cha-**Cmd**

Table 1: Sequences of some phytochelatin-related α-peptides. [a] 100 mM PBS buffer pH 7.2.[b]25 mM potassium hydrophthalate buffer pH 4.0 and 25 mM sodium bicarbonate buffer pH 10.0. [c]All sequences are written from N- to C-terminus. Cmd: carboxamide; Ac: N-terminal acetylation; Suc: N-terminal succinylation; Cha: 3-cyclohexylalanine, PEG: hexaethyleneglycol. ND: not determined. From ref. [1].

Peptide **1** (Table 1), composed of the adhesive domain only, could efficiently solubilize CdSe/ZnS in DMSO and water but the aggregates were observed at pH 7.2 in phosphate buffer saline (PBS) buffers for concentration above 5 mM. The addition of a polar second domain, such as that of peptide **2**, enhanced the stability in PBS buffers with ionic strength up to 20 mM, although small NCs aggregates formed above this molarity. When positive charges were added by means of arginine residues (R) (peptide **3**) to improve the stability of the particles in higher ionic strength buffers, the NCs readily aggregated upon water solubilization. These aggregations may have arisen from the interaction of the positively charged arginine residues with the negatively charged surface of the NCs. To overcome these charge interactions, a polar but negatively charged domain containing glutamic acid residues (E) (peptide **4**) was tested, and successfully conferred both solubilization and colloidal stability to the nanoparticles in PBS buffers containing 100 mM and higher salt. This domain was thus chosen as a *hydrophilic linker* addition for other peptides sequences (Fig. 1A).

2.3. Modularity of the peptide toolkit

The peptide code has a few billion years of proven record of versatility, and modern peptide synthesis techniques allow a relatively simple strategy of rational design and parallel synthesis to explore it in a targeted manner. Starting from the

two basic building blocks (or modules) presented previously: (i) an adhesive domain, and (ii) a hydrophilic linker, it is possible to build more complex sequences providing functional handles to the coated-NC. A set of possible examples, some actually used in our laboratory, and some easily obtainable with current techniques, is depicted schematically in Fig. 1B. Cationic peptide sequences derived from the HIV Tat protein[48] or other protein transduction domains (PTD) have been shown to promote cellular uptake of large molecules including nanocrystals[24], and could be efficiently used as a cellular *entry module*. For delivery to specific cellular compartment, peptide recognition sequences (R in Fig. 1B) are natural candidates for targeting as demonstrated by nanocrystal labeling of mitochondria[49] or the nucleus[49, 50]. Clivable sequences, peptide "velcros", and even small proteins can be added to the sequences used to complement the adhesive and hydrophilic liner modules of the peptide toolkit. The first example is illustrated in Fig. 1B with a quencher sequence (Q) that can be released by enzyme clivage, reporting on the presence of this enzyme by turning-on of the NC fluorescence.

When specific functions cannot be easily provided by mere peptide add-ons, chemical moieties can be attached to the basic building block, as illustrated for instance by the biotin-peptide (B) and the PEG-peptide coatings (P). Polyethyleneglycol (PEG) is known to prevent non-specific adhesion of various type of particles (and NCs) to biological substrates and has been successfully used to prevent rapid elimination of injected NCs from the blood circulation[2]. Another type of modification by small chemical is illustrated by the addition of DOTA, a metal chelator used in radiolabeling studies (D, see also section 6), which allows both fluorescence and PET techniques to be used with a single probe.

3. COLLOIDAL PROPERTIES OF PEPTIDE-COATED NANOCRYSTALS

Peptide-coated NCs are stable for months at room temperature and in buffers with biologically relevant ionic strength. More specifically, their excellent size distribution (see below) remains stable, which is a prerequisite for the simple interpretation of biological observations where aggregation can be observed.

3.1. Size distribution as measured by standard techniques

Synthesis of NC cores often result in size dispersion of a few percents only[51], with a slight broadening upon overcoating by a few shell layer[52-54], as measured by transmission electron microscopy (TEM). This small dispersion results in the characteristic narrow emission spectra of NCs. The size dispersion of functionalized NCs is not has easily measured, since the organic material does not offer any electronic contrast. Staining with heavy elements can solve this problem[13, 36], but this approach is not simple or even guaranteed to succeed. A more standard method consist of taking advantage of the solubility of functionalized NCs, and use SE-HPLC or gel electrophoresis to monitor the size distribution of the sample. Fig. 2 illustrates the extraordinary narrow distribution of the peptide-coated NCs and the flexibility of the peptide coating.

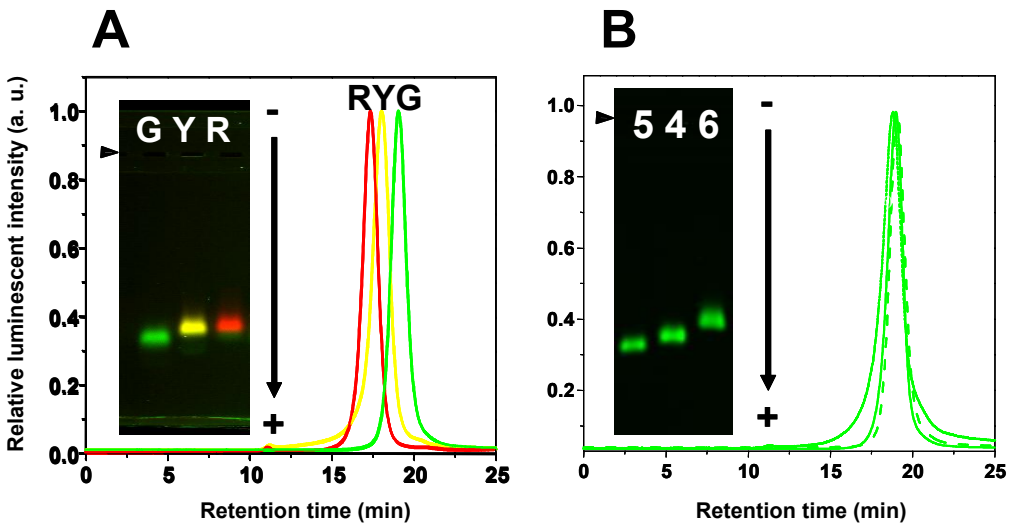

Fig. 2: SEC HPLC and gel electrophoresis of peptide-coated CdSe/ZnS nanocrystals. A. Effect of NC size. Green, yellow and red NCs emitting at 530, 565 and 617 nm respectively and coated with peptide 5 were separated on a size exclusion column against a 0.1 M PBS mobile phase. The diameter of the peptide-coated NCs was evaluated from the elution times as 129.4 Å (±15%), 150.3 Å (±16%) and 164.8 Å (±14%) respectively. Inset: 0.5 % agarose gel electrophoresis of the same three peptide-coated NCs samples in TBE buffer pH 8.3. B. Effect of peptide charge. NCs coated with peptide **5** (dash), peptide **4** (dot) or peptides **6** (solid) have similar retention times on a SEC HPLC column. Inset: the same peptide-

coated NCs migrate at different positions on a 0.5 % agarose gel, in good agreement with the theoretical charge of each peptide. -►: position of the loading wells. →: direction of the applied electric field. Adapted from ref. [1].

Fig. 2A shows that a single type of peptide will not interfere with the expected order of migration, demonstrating a constant peptide layer thickness, whatever the original size of the nanoparticle. Fig. 2B on the other hand, shows that peptides with identical length but different electric charges will result in different coatings of the same underlying nanoparticle. SE-HPLC provides an estimate of the hydrodynamic radius of the coated nanoparticle. Assuming that this can be identified with the radius of the particle, the measured thickness of the peptide layer is 4.6 nm is in good agreement with what is expected from a 10 aminoacid-long peptide chain [1]. Interstingly, this result cannot be obtained with atomic force microscopy, due to the different tip-sample interactions between TOPO-coated NCs and peptide-coated NCs[1].

3.2. The verdict of fluorescence correlation spectroscopy

Fluorescence correlation spectroscopy (FCS) has become a method of choice to study small molecules in solution[55]. It has recently been applied to NC in a 2-photon excitation (2-PE) mode[56] to study emission saturation and differences in diffusion coefficients (a measure of particle size) between organic solvent and water soluble NCs. We have systematically investigated NC produced in our laboratory using 1-PE FCS in order to characterize their photophysics and size before and after solubilization[57]. An estimate of the size can be obtained from the hydrodynamic radius R calculated by the Stokes-Einstein equation: $R = k_B T \big/ 6\pi\eta D$ where η is the viscosity and D the measured diffusion constant. Fig. 3A-B show a comparison of results obtained for different type of solubilization approaches and different NCs emitting at around the same wavelength (~ 600 nm), together with a bead sample of precisely know diameter (26 nm) as control. The interesting observation is that the peptide coating results in the smallest particles (~12 nm, compared to ~18 nm for phospholipid-coated NCs, and 30 nm for commercial nanorods protected by a polymer coat). This is definitely an advantage for cell biology applications in which interference with biological interactions and target inaccessibility due to steric hindrance need to be kept to a minimum.

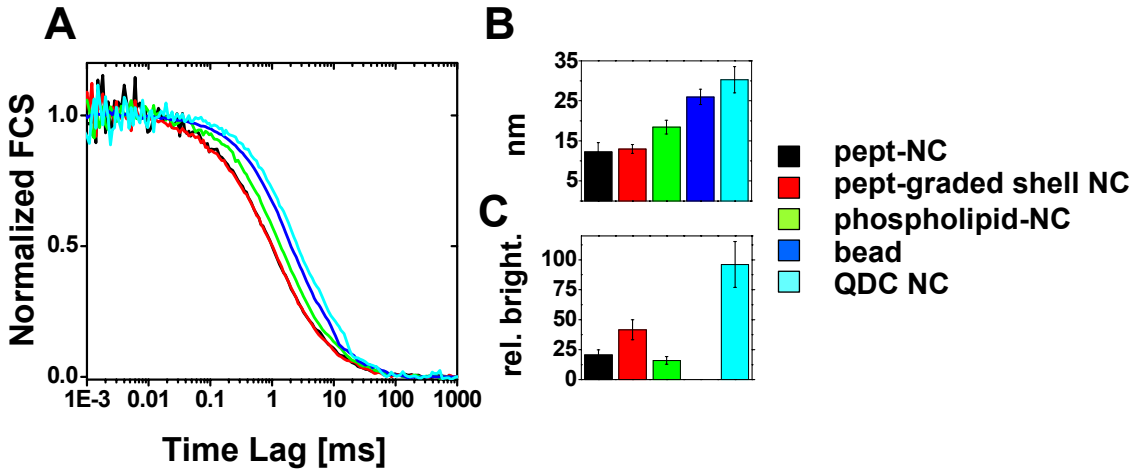

Fig. 3: Comparative fluorescence correlation spectroscopy (FCS) analysis of nanocrystals. A. Normalized FCS curves of different nanocrystal preparations, and comparison with fluorescent beads. Color coding: black: peptide-coated CdSe/ZnS, red: peptide-coated CdSe/ZnCdS, green: phospholipids coated CdSe/ZnS (prepared as in ref. [13]), dark blue: 25 nm bead, light blue: 605 nm emitting NCs from Quantum Dot Corp. The NCs and beads were chosen to emit at similar wavelengths (~600 nm). The FCS curve fit provides two parameters: the diffusion time, and the number of particle per excitation volume. From these and other information, the hydrodynamic diameter of the particles (B) and the brightness per particle in percent (C) can be deduced[57].

4. PHOTOHYSICAL PROPERTIES OF PEPTIDE-COATED NANOCRYSTALS

An almost universal observation of researchers in the field is the loss of quantum yield (QY) of NCs upon solubilization. This fate was not spared to the first peptide-coated NCs produced in our laboratory. Quantum yield is

however an ensemble measurement that does not report adequately on the individual brightness per particle, *b*. This quantity can be obtained from FCS measurements as: $b = I/N$, where I is the average signal, and N the occupancy of the excitation volume is given by the inverse amplitude of the FCS curve: $N = 1/g^{(2)}(0)$. Measured at the same intensity for different samples, it gives a measure of the relative brightness of the fraction of emitting particles in the sample[57]. This fraction can be low[58], and this will reduce the observed QY. Fig. 3C represents the result of measurements of b/b_0 for the different samples, where b_0 is the largest measured brightness per particle. Note that b_0 corresponds to rods that may have a comparatively larger absorption cross-section. Two parameters can thus be improved in a NC sample: (i) the brightness per particle, and (ii) the fraction of emitting particles.

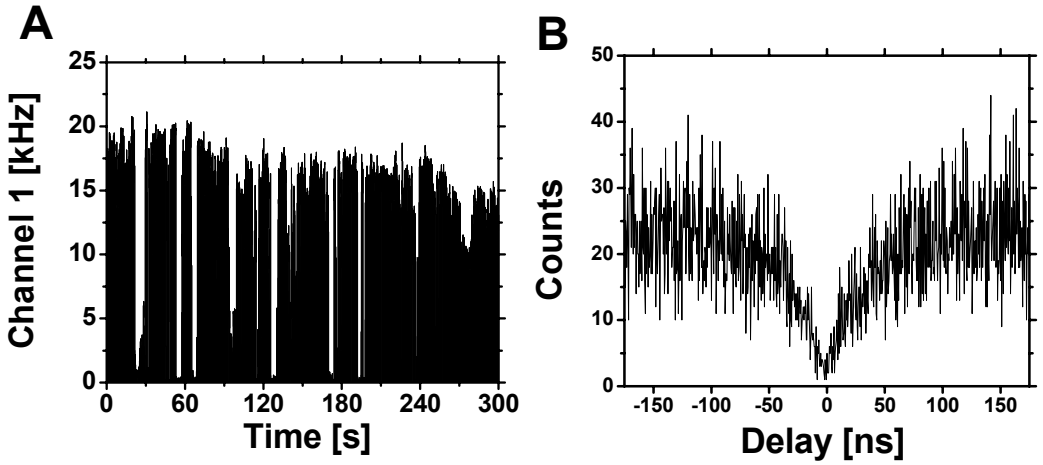

Fig. 4: Single-molecule spectroscopy of peptide-coated NCs. A: Time trace of fluorescence emission of a red peptide-coated NC observed by confocal microscopy (see ref. [59] for setup details), exhibiting intermittency. Excitation: 100 nW at 488 nm. Detection: the signal was equally split by a non-polarizing beam splitter cube and sent to two avalanche photodiodes. The signal of a single channel is shown here. B: Antibunching histogram corresponding to the time trace shown in (A) obtained using a setup similar as described in ref. [60]. The histogram represents the delay between successive photons emitted by the observed nanocrystal, as detected by the two detectors (start and stop). The absence of events with zero-delay indicates the presence of a single emitter. This histogram thus confirms that the trace in (A) corresponds to a single weakly blinking NC.

The well known intermittent fluorescence of NCs (Fig. 4A) suggests a possible way to improve brightness per particle: by reducing the amount of blinking, the total number of photons per unit time can be increased without any need to increase the maximum emission rate of NCs. A recent report[61] seems to indicate that thiol groups contribute to a quenching of electron traps on the NC surface. The presence of six thiol moieties per adhesive module in our peptide coating could thus explain the relative low blinking observed in Fig. 4A (see also Fig. 5).

Sample	Emission Peak		QY	
	TOP/TOPO (toluene)	peptides (water)	TOP/TOPO (toluene)	peptides (water)
CdSe/ZnS	613	613	19%	9-15%
CdSe/CdS/ZnS (graded)	620	625-630	26%	20-35%
CdSe/CdS/ZnS (layered)	622	624-625	14%	1-2%
CdSe/CdS	620	622-623	35%	2-3%
CdSe/CdS/ZnS (graded)	648	652-654	16%	10-13%

Table 2: CdSe cores over-coated with inorganic shells of various compositions at different stages of peptide exchange. All quantum dots (1-3) have identical core sizes (4.5 nm) except sample 4 (CdSe/CdS, 3.5 nm core) Sample 5 has a 5 x 25 nm core.

Beyond this beneficial effect of peptide coating, we studied possible modifications to the NC shell structure that could enhance their luminescence[62]. Reports of increased QY in NC samples possessing a graded CdS/ZnS shell[63] with reduced lattice mismatch led us to look at the cumulated effects of graded/layered shells and peptide coating. Table 2 summarizes our results: peptide-coating and UV annealing of a simple of graded shell allows an almost complete recovery of the original QY, with the graded shell resulting in the higher QY. An additional effect worth noticing is the slight red shift of the emission spectra upon peptide-coating of the graded and layered shell samples, indicating a possible interaction between the excitonic wavefunction and the peptide molecular orbitals. Experiments performed

with peptide sequences containing the same adhesive module and different hydrophilic linkers showed no differences, indicating that only the amino-acids in close contact with the shell play a role in this spectral shift. We are currently investigating other adhesive sequences to further quantify this phenomenon.

5. SINGLE-PARTICLE TRACKING OF MEMBRANE RECEPTORS IN LIVE CELLS

Among the non-peptide module depicted in Fig. 1B, biotin is one of the simplest and most potent functions that can be added to NCs. Its high affinity for avidin or streptavidin makes it a tool of choice for many biochemical assays. We discovered that peptide-coated NCs non-specifically bind to avidin *in vitro*, but not *in vivo*, whereas this non-specificity is absent for streptavidin and neutravidin[1]. To validate the biocompatibility of the biotinylated peptide-coated NCs (bpc-NCs), we targeted them to the cell membrane of HeLa cells over-expressing a GPI-anchored avidin-CD14 (av-CD14) chimeric receptor protein[1] (CD14 is not constitutively expressed by HeLa cells). Controls showed that the binding was specific of the cells expressing the mutant receptor and of the bpc-NCs. At high concentration of bpc-NCs, we observed rapid internalization of the bpc-NCs in the perinuclear region, in agreement with control experiments performed with Alexa 594 biocytin using standard epifluorescence microscopy[1].

At very low concentration of bpc-NCs however, we were able to observe individual binding events and the subsequent Brownian motion of individually labeled Av-CD14 receptors, as illustrated in Fig. 5. The brightness and high saturation intensity of peptide-coated NCs[57, 62] allows the use of an inexpensive CCD camera (CoolSnap *cf*, Princeton Instruments, Trenton, NJ) and rather short exposure (100 ms). Later experiments performed with an electron multiplying camera (Cascade 512B, Princeton Intruments) and total internal reflection (TIR) microscopy allowed using much shorter exposure time (20 ms or less). As mentioned previously, peptide-coated NC exhibited very little blinking and negligible bleaching (Fig. 5D), permitting long-term tracking of individual particles. These long trajectories give access to a wealth of information on the local spatio-temporal environment of each particle, which would be accessible only through statistical analysis of hundreds of trajectories using standard fluorescent dyes[64]. We are currently studying the association of individual receptors with lipid rafts using this very powerful new tool.

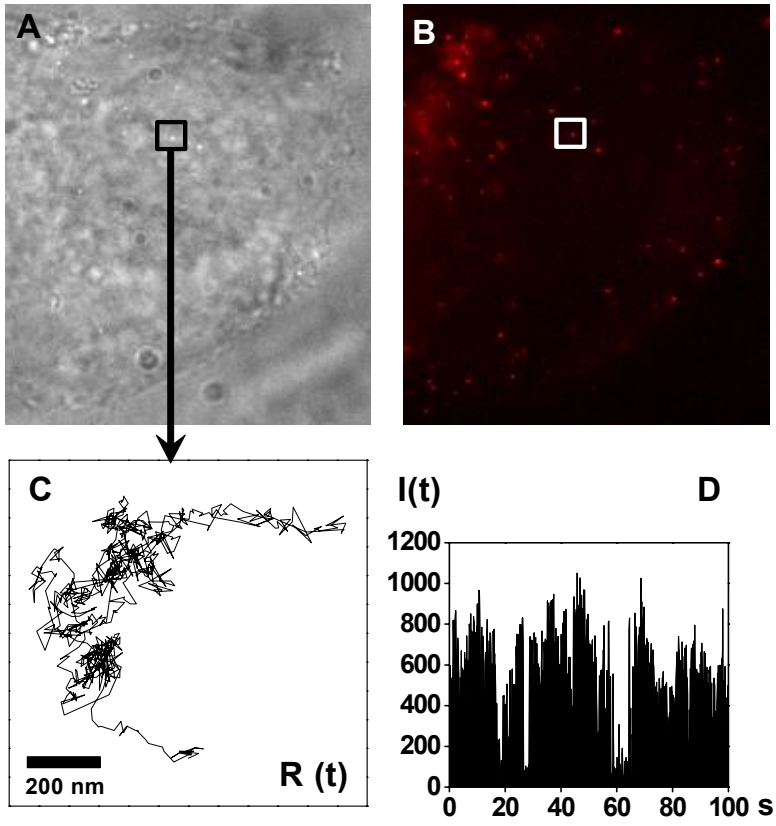

Fig. 5: Single-particle tracking in a live-cell. The brightness and photostability of NCs permits single NC observation over a long period of time. Live HeLa cells stably transfected with a plasmid expressing a chimeric avidin-CD14 receptor[1] were grown on fibronectin-coated glass coverslips, incubated with biotin-NCs (emission: 630 nm), and washed with the observation medium. The cells were observed in DIC (A) and epifluorescence (B) on an inverted microscope (Axiovert 100, Zeiss) using a simple Hg lamp and imaged with a cooled monochrome CCD camera (CoolSnap HQ, Roper Scientific). Single-NCs were observed to diffuse at characteristically different rates in different regions of the membrane or inside the cytosol (data not shown). C: The 1,000 steps (100 ms/step) trajectory, R(t), of the NC localized in the region marked in panel (A, B), with (D) the corresponding NC intensity, I(t). The blinking pattern (succession of on and off emission) demonstrates that a single NC was observed. From ref. [4].

6. FLUORESCENCE AND μPET IN LIVE ANIMALS

Besides their exceptional fluorescence characteristics, the large electronic density of NCs makes them excellent TEM probes, as demonstrated by recent dual fluorescence/TEM studies[34]. This gives access to the high-resolution spatial and temporal information afforded by single-molecule fluorescence tracking, but also to the very high-resolution structural information, unique to electron microscopy. Fluorescence NCs however have also proven their value in a multitude of live animal studies, in which near-infrared emitting NCs were injected and imaged through the animal skin[10] or used as a background-free reporter for surgery[65]. Deeper imaging might however be difficult to perform, due to absorption and scattering of the excitation and emission light.

We therefore explored another route, using microPET imaging of NCs injected in the blood circulation (Fig. 6A). NCs having DOTA (a chelator used for radiolabeling) and 600 Da PEG on their surface were radiolabeled with ^{64}Cu (a positron-emitting isotope with a 12.7 hour half-life). These NCs were then injected (~ 80 uCi per animal) via tail-vein into nude mice under anesthesia and imaged in a small animal scanner at regular intervals. Rapid and marked accumulation of NCs in the liver quickly follows their intravenous injection in normal adult nude mice. The liver is the single largest organ that traps the majority of the injected NCs. The uptake of NCs by Kupffer cells that are part of the reticulo-endothelial system in the liver is the likely reason for the high accumulation of radiolabeled NCs in the hepatic region, which could be prevented by using higher molecular weight PEG-peptide coating. Biopsies of the liver observed by optical microscopy, confirm this accumulation of NCs within hepatocytes (Fig. 6B). A further step could involve TEM imaging of the precise localization of NCs in cells, illustrating the potential of NCs as probes at the macro-, micro- and nanoscale.

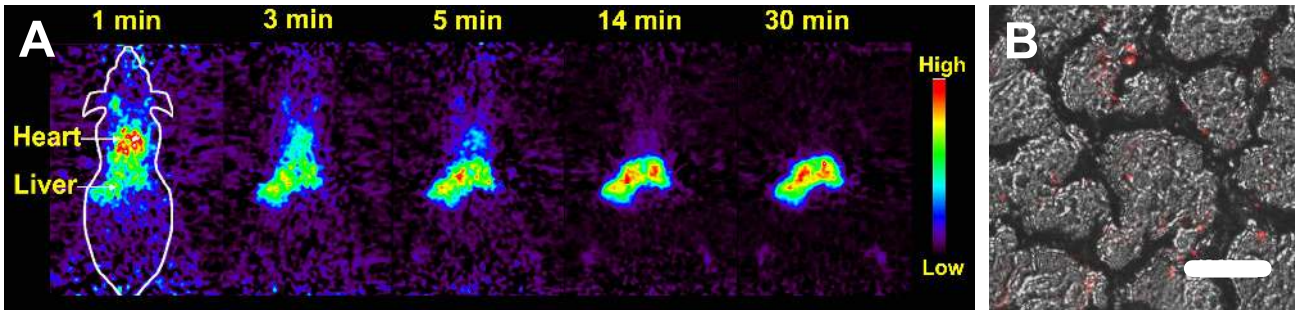

Fig. 6: microPET imaging of NCs. NCs having DOTA (a chelator used for radiolabeling) and 600 dalton PEG on their surface were radiolabeled with ^{64}Cu (positron-emitting isotope with 12.7 hour half-life). These NCs were then injected via tail-vein into nude mice (~ 80 uCi per animal) and imaged in a small animal scanner. A: Rapid and marked accumulation of NCs in the liver quickly follows their intravenous injection in normal adult nude mice. This could be avoided by functionalizing NCs with higher molecular weight PEG chains, as demonstrated in other studies[2]. B: Overlay of DIC and fluorescence images of hepatocytes from a mouse showing the accumulation of NCs within liver cells. Scale bar indicates 20 um. Adapted from ref. [4].

7. CONCLUSION AND PERSPECTIVES

We have developed a novel approach for the solubilization and functionalization of NCs, and demonstrated its potential for biological imaging, both at the single-molecule level in live cell and in whole live animal. The resulting NCs are not only very monodisperse, but they remain of moderate size, have quantum yields comparable to the original non-functionalized NCs and moderate blinking. The peptide toolkit has the advantage to produce bioactivated particles in a single step, and offer the modularity of the peptide code, while leaving open the possibility to attach any desirable chemical moiety to the peptide coat. We are working on applications of this technology to fluorescence in situ hybridization, intracellular targeting and to extend it to NCs with different composition.

8. ACKNOWLEDGMENTS

We are grateful to our current and former colleagues: J. Antelman, S. Prasad, D. Majumdar, B. Campbell, for their support during the course of this work. Some of the results presented here are the fruits of collaborations with other

researchers: H.-P. Moore, D. King, E. Margeat, T. Olafsen, A.M. Wu, G. Sundaresan and S. S. Gambhir. This work was supported by the NIH (grant 5-R01-EB000312), the Keck Foundation (grant 04074070) and DARPA/AFOSR (grant FA955004-10048).

9. REFERENCES

1. F. Pinaud, D. King, H.-P. Moore, and S. Weiss, "Bioactivation and Cell Targeting of Semiconductor CdSe/ZnS Nanocrystals with Phytochelatin-Related Peptides," J. Am. Chem. Soc. **126**, 6115-6123 (2004).
2. B. Ballou, B. C. Lagerholm, L. A. Ernst, M. P. Bruchez, and A. S. Waggoner, "Noninvasive imaging of quantum dots in mice," Bioconjug. Chem. **15**(1), 79-86 (2004).
3. A. P. Alivisatos, "Semiconductor Clusters, Nanocrystals, and Quantum Dots," Science **271**(5251), 933-937 (1996).
4. X. Michalet, F. F. Pinaud, L. A. Bentolila, J. M. Tsay, S. Doose, J. J. Li, G. Sundaresan, A. M. Wu, S. S. Gambhir, and S. Weiss, "Quantum Dots for Live Cells, in Vivo Imaging and Diagnostics," Science **306**, ??? (2005).
5. W. C. W. Chan and S. M. Nie, "Quantum dot bioconjugates for ultrasensitive nonisotopic detection," Science **281**(5385), 2016-2018 (1998).
6. S. Pathak, S. K. Choi, N. Arnheim, and M. E. Thompson, "Hydroxylated quantum dots as luminescent probes for in situ hybridization," J. Am. Chem. Soc. **123**(17), 4103-4104 (2001).
7. S. Kim and M. G. Bawendi, "Oligomeric Ligands for luminescent and stable nanocrystal quantum dots," J. Am. Chem. Soc. **125**(48), 14652-14653 (2003).
8. W. Guo, J. J. Li, Y. A. Wang, and X. G. Peng, "Conjugation chemistry and bioapplications of semiconductor box nanocrystals prepared via dendrimer bridging," Chem. Mater. **15**(16), 3125-3133 (2003).
9. X. Y. Wu, H. J. Liu, J. Q. Liu, K. N. Haley, J. A. Treadway, J. P. Larson, N. F. Ge, F. Peale, and M. P. Bruchez, "Immunofluorescent labeling of cancer marker Her2 and other cellular targets with semiconductor quantum dots," Nature Biotechnol. **21**(1), 41-46 (2003).
10. X. Gao, Y. Cui, R. M. Levenson, L. W. K. Chung, and S. Nie, "In vivo cancer targeting and imaging with semiconductor quantum dots," Nature Biotechnol. **22**, 969 (2004).
11. M. Bruchez, M. Moronne, P. Gin, S. Weiss, and A. P. Alivisatos, "Semiconductor nanocrystals as fluorescent biological labels," Science **281**(5385), 2013-2016 (1998).
12. D. Gerion, F. Pinaud, S. C. Williams, W. J. Parak, D. Zanchet, S. Weiss, and A. P. Alivisatos, "Synthesis and properties of biocompatible water-soluble silica-coated CdSe/ZnS semiconductor quantum dots," J. Phys. Chem. B **105**(37), 8861-8871 (2001).
13. B. Dubertret, P. Skourides, D. J. Norris, V. Noireaux, A. H. Brivanlou, and A. Libchaber, "In vivo imaging of quantum dots encapsulated in phospholipid micelles," Science **298**(5599), 1759-1762 (2002).
14. X. Gao, W. C. W. Chan, and S. Nie, "Quantum-dot nanocrystals for ultrasensitive biological labeling and multicolor optical encoding," J. Biomed. Opt. **7**(4), 532-537 (2002).
15. T. Pellegrino, L. Manna, S. Kudera, T. Liedl, D. Koktysh, A. L. Rogach, S. Keller, J. Radler, G. Natile, and W. J. Parak, "Hydrophobic nanocrystals coated with an amphiphilic polymer shell: A general route to water soluble nanocrystals," Nano Lett. **4**(4), 703-707 (2004).
16. F. Osaki, T. Kanamori, S. Sando, T. Sera, and Y. Aoyama, "A Quantum Dot Conjugated Sugar Ball and Its Cellular Uptake. On the Size Effects of Endocytosis in the Subviral Region," J. Am. Chem. Soc. **126**, 6520-6521 (2004).
17. D. M. Willard, L. L. Carillo, J. Jung, and A. Van Orden, "CdSe-ZnS quantum dots as resonance energy transfer donors in a model protein-protein binding assay," Nano Lett. **1**(9), 469-474 (2001).
18. H. Mattoussi, J. M. Mauro, E. R. Goldman, G. P. Anderson, V. C. Sundar, F. V. Mikulec, and M. G. Bawendi, "Self-assembly of CdSe-ZnS quantum dot bioconjugates using an engineered recombinant protein," J. Am. Chem. Soc. **122**(49), 12142-12150 (2000).
19. A. Sukhanova, M. Devy, L. Venteo, H. Kaplan, M. Artemyev, V. Oleinikov, D. Klinov, M. Pluot, J. H. M. Cohen, and I. Nabiev, "Biocompatible fluorescent nanocrystals for immunolabeling of membrane proteins and cells," Anal. Biochem. **324**(1), 60-67 (2004).
20. A. L. Rogach, M. T. Harrison, S. V. Kershaw, A. Kornowski, M. G. Burt, A. Eychmuller, and H. Weller, "Colloidally prepared CdHgTe and HgTe quantum dots with strong near-infrared luminescence," Phys. Status Solidi B **224**(1), 153-158 (2001).
21. N. Gaponik, D. V. Talapin, A. L. Rogach, K. Hoppe, E. V. Shevchenko, A. Kornowski, A. Eychmüller, and H. Weller, "Thiol-capping of CdTe nanocrystals: an alternative to organometallic synthetic routes," J. Phys. Chem. B **106**, 7177-7185 (2002).

22. L. Wenhua, X. Haiyan, X. Zhixiong, L. Zhexue, O. Jianhong, C. Xiangdong, and S. Ping, "Exploring the mechanism of competence development in *Escherichi coli* using quantum dots as fluorescent probes," J. Biochem. Biophys. Meth. **58**, 59-66 (2004).
23. J. K. Jaiswal, H. Mattoussi, J. M. Mauro, and S. M. Simon, "Long-term multiple color imaging of live cells using quantum dot bioconjugates," Nature Biotechnol. **21**(1), 47-51 (2003).
24. L. C. Mattheakis, J. M. Dias, Y. J. Choi, J. Gong, M. P. Bruchez, J. Liu, and E. Wang, "Optical coding of mammalian cells using semiconductor quantum dots," Anal. Biochem. **327**(2), 200-208 (2004).
25. T. Pellegrino, W. J. Parak, R. Boudreau, M. Le Gros, D. Gerion, A. P. Alivisatos, and C. Larabell, "Quantum dot-based cell motility assay," Differentiation **71**, 542-548 (2003).
26. F. Patolsky, R. Gill, Y. Weizmann, T. Mokari, U. Banin, and I. Willner, "Lighting-up the dynamics of telomerization and DNA replication by CdSe-ZnS quantum dots," J. Am. Chem. Soc. **125**(46), 13918-13919 (2003).
27. M. E. Akerman, W. C. W. Chan, P. Laakkonen, S. N. Bhatia, and E. Ruoslahti, "Nanocrystal targeting in vivo," Proc. Natl. Acad. Sci. USA **99**(20), 12617-12621 (2002).
28. G. P. Mitchell, C. A. Mirkin, and R. L. Letsinger, "Programmed assembly of DNA functionalized quantum dots," J. Am. Chem. Soc. **121**(35), 8122-8123 (1999).
29. B. Q. Sun, W. Z. Xie, G. S. Yi, D. P. Chen, Y. X. Zhou, and J. Cheng, "Microminiaturized immunoassays using quantum dots as fluorescent label by laser confocal scanning fluorescence detection," J. Immun. Meth. **249**(1-2), 85-89 (2001).
30. E. R. Goldman, G. P. Anderson, P. T. Tran, H. Mattoussi, P. T. Charles, and J. M. Mauro, "Conjugation of luminescent quantum dots with antibodies using an engineered adaptor protein to provide new reagents for fluoroimmunoassays," Anal. Chem. **74**(4), 841-847 (2002).
31. E. R. Goldman, A. R. Clapp, G. P. Anderson, H. T. Uyeda, J. M. Mauro, I. L. Medintz, and H. Mattoussi, "Multiplexed toxin analysis using four colors of quantum dot fluororeagents," Anal. Chem. **76**(3), 684-688 (2004).
32. J. M. Ness, R. S. Akhtar, C. B. Latham, and K. A. Roth, "Combined tyramide signal amplification and quantum dots for sensitive and photostable immunofluorescence detection," J. of Histochem. Cytochem. **51**(8), 981-987 (2003).
33. G. D. Bachand, S. B. Rivera, A. K. Boal, J. Gaudioso, J. Liu, and B. C. Bunker, "Assembly and Transport of Nanocrystal CdSe Quantum Dot Nanocomposites Using Microtubules and Kinesin Motor Proteins," Nano Lett. **4**(5), 817-821 (2004).
34. M. Dahan, S. Levi, C. Luccardini, P. Rostaing, B. Riveau, and A. Triller, "Diffusion dynamics of glycine receptors revealed by single-quantum dot tracking," Science **302**(5644), 442-445 (2003).
35. A. Mansson, M. Sundberg, M. Balaz, R. Bunk, I. A. Nicholls, P. Omling, S. Tagerud, and L. Montelius, "In vitro sliding of actin filaments labelled with single quantum dots," Biochem. Biophys. Res. Commun. **314**(2), 529-534 (2004).
36. D. Ishii, K. Kinbara, Y. Ishida, N. Ishii, M. Okochi, M. Yohda, and T. Aida, "Chaperonin-mediated stabilization and ATP-triggered release of semiconductor nanoparticles," Nature **423**(6940), 628-632 (2003).
37. C. T. Dameron, R. N. Reese, R. K. Mehra, A. R. Kortan, C. P. J., M. L. Steigerwald, L. E. Brus, and D. R. Winge, "Biosynthesis of cadmium sulphide quantum semiconductor crystallites," Nature **338**, 596-597 (1989).
38. S. R. Whaley, D. S. English, E. L. Hu, P. F. Barbara, and A. M. Belcher, "Selection of peptides with semiconductor binding specificity for directed nanocrystal assembly," Nature **405**(6787), 665-668 (2000).
39. C. Mao, C. E. Flynn, A. Hayhurst, R. Sweeney, J. Qi, G. Georgiou, B. Iverson, and A. M. Belcher, "Virus-based toolkit for the directed synthesis of magnetic and semiconducting nanowires," Science **303**(5655), 213-217 (2004).
40. C. S. Cobbett, "Heavy Metal Detoxification in Plants: Phytochelatin Biosynthesis and Function," IUBMB Life **51**(3), 183-188 (2001).
41. C. T. Dameron and D. R. Winge, "Peptide-mediated formation of quantum semiconductors," Trends in Biotechnology **8**, 3-6 (1990).
42. C. T. Dameron and D. R. Winge, "Characterization of Peptide-Coated Cadmium-Sulfide Crystallites," Inorganic Chemistry **29**, 1343-1348 (1990).
43. W. Bae, R. Abdullah, D. Henderson, and R. K. Mehra, "Characteristics of glutathione-capped ZnS nanocrystallites," Biochem. Biophys. Res. Commun. **237**(1), 16-23 (1997).
44. J. M. Whitling, G. Spreitzer, and D. W. Wright, "A Combinatorial and Informatics Approach to CdS Nanoclusters," Adv. Mater. **12**(18), 1377-1380 (2000).
45. G. Spreitzer, J. M. Whitling, J. D. Madura, and D. W. Wright, "Peptide-encapsulated CdS nanoclusters from a combinatorial ligand library," Chem. Comm. **3**, 209-210 (2000).

46. A. Sukhanova, L. Venteo, J. Devy, M. Artemyev, V. Oleinikov, M. Pluot, and I. Nabiev, "Highly Stable Fluorescent Nanocrystals as a Novel Class of Labels for Immunohistochemical Analysis of Paraffin-Embedded Tissue Sections," Laboratory Investigation **82**(9), 1259 (2002).
47. W. Bae and R. K. Mehra, "Cysteine-capped ZnS nanocrystallites: Preparation and characterization," Journal of Inorganic Biochemistry **70**(2), 125-135 (1998).
48. S. Futaki, "Structural variety of membrane permeable peptides," Curr. Protein Pept. Sci. **4**(2), 87-96 (2003).
49. A. M. Derfus, W. C. W. Chan, and S. N. Bhatia, "Intracellular delivery of quantum dots for live cell labeling and organelle tracking," Adv. Mater. **16**(12), 961-966 (2004).
50. F. Chen and D. Gerion, "Fluorescent CdSe/ZnS Nanocrystal-Peptide Conjugates for Long-term, Nontoxic Imaging and Nuclear Targeting in Living Cells," Nano Lett. **4**(10), 1827-1832 (2004).
51. C. B. Murray, D. J. Norris, and M. G. Bawendi, "Synthesis and Characterization of Nearly Monodisperse CdE (E = S, Se, Te) Semiconductor Nanocrystallites," Journal of the American Chemical Society **115**, 8706-8715 (1993).
52. M. A. Hines and P. Guyot-Sionnest, "Synthesis and characterization of strongly luminescing ZnS-capped CdSe nanocrystals," Journal of Physical Chemistry **100**, 468-471 (1996).
53. R. O. Dabbousi, J. Rodriguez-Viejo, F. V. Mikulec, J. R. Heine, H. Mattoussi, R. Ober, K. F. Jensen, and M. G. Bawendi, "(CdSe)ZnS Core-Shell Quantum Dots: Synthesis and Characterization of a Size Series of Highly Luminescent Nanocrystallites," Journal of Physical Chemistry B **101**, 9463-9475 (1997).
54. X. G. Peng, M. C. Schlamp, A. V. Kadavanich, and A. P. Alivisatos, "Epitaxial growth of highly luminescent CdSe/CdS core/shell nanocrystals with photostability and electronic accessibility," Journal of the American Chemical Society **119**(30), 7019-7029 (1997).
55. R. Rigler and E. S. Elson, eds., *Fluorescence Correlation Spectroscopy. Theory and Applications*, Chemical Physics (Springer, 2001).
56. D. Larson, W. Zipfel, R. Williams, S. Clark, M. Bruchez, F. Wise, and W. W. Webb, "Water-soluble quantum dots for multiphoton fluorescence imaging in vivo," Science **300**, 1434-1436 (2003).
57. S. Doose, J. M. Tsay, F. F. Pinaud, and S. Weiss, "Comparison of Photophysical and Colloidal Properties of Biocompatible Semiconductor Nanocrystals Using Fluorescence Correlation Spectroscopy," submitted (2005).
58. Y. Ebenstein, T. Mokari, and U. Banin, "Fluorescence quantum yield of CdSe/ZnS nanocrystals investigated by correlated atomic-force and single-particle fluorescence microscopy," Appl. Phys. Lett. **80**(21), 4033 (2002).
59. T. D. Lacoste, X. Michalet, F. Pinaud, D. S. Chemla, A. P. Alivisatos, and S. Weiss, "Ultrahigh-resolution multicolor colocalization of single fluorescent probes," Proc. Natl. Acad. Sci. USA **97**(17), 9461-9466 (2000).
60. B. Lounis, H. A. Bechtel, D. Gerion, A. P. Alivisatos, and W. E. Moerner, "Photon antibunching in single CdSe/ZnS quantum dot fluorescence," Chem. Phys. **329**, 399-404 (2000).
61. S. Hohng and T. Ha, "Near-complete suppression of quantum dot blinking in ambient conditions," J. Am. Chem. Soc. **126**(5), 1324-1325 (2004).
62. J. M. Tsay, S. Doose, F. F. Pinaud, and S. Weiss, "Enhancing the photoluminescence of peptide-coated CdSe nanocrystals with shell composition and UV irradiation," J. Phys. Chem. (in press)(2005).
63. L. Manna, E. C. Scher, L. S. Li, and A. P. Alivisatos, "Epitaxial growth and photochemical annealing of graded CdS/ZnS shells on colloidal CdSe nanorods," J. Am. Chem. Soc. **124**(24), 7136-7145 (2002).
64. T. Schmidt, G. J. Schütz, W. Baumgartner, H. J. Gruber, and H. Schindler, "Imaging of single molecule diffusion," Proceedings of the National Academy of Sciences USA **93**, 2926-2929 (1996).
65. S. Kim, Y. T. Lim, E. G. Soltesz, A. M. De Grand, J. Lee, A. Nakayama, J. A. Parker, T. Mihaljevic, R. G. Laurence, D. M. Dor, L. H. Cohn, M. G. Bawendi, and J. V. Frangioni, "Near-infrared fluorescent type II quantum dots for sentinel lymph node mapping," Nature Biotechnol. **22**(1), 93-97 (2004).